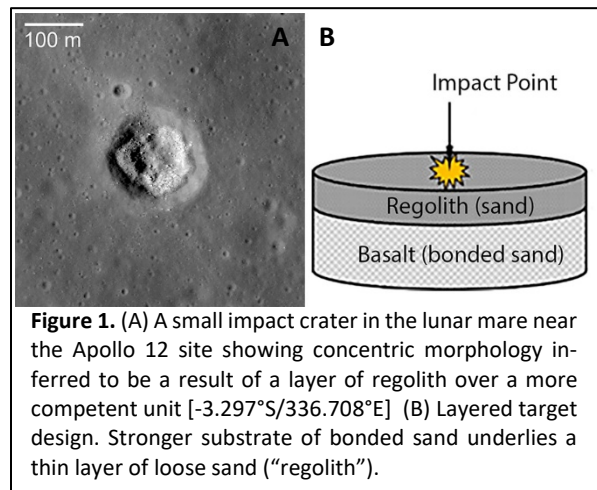


Experimental Impacts into Strength-Layered Targets: Crater Morphology and Morphometry. J.L.B. Anderson¹, L.E. Dechant¹, C.J. Cline II², R.A. Taitano¹, J.M. Ebel¹, M.J. Cintala³, J.B. Plescia⁴. ¹Geoscience, Winona State Univ., Winona, MN 55987. ²Jacobs, NASA Johnson Space Center, Houston, TX 77058. ³Code XI3, NASA Johnson Space Center, Houston, TX 77058. ⁴Applied Physics Lab, Johns Hopkins Univ., Laurel, MD 20723. (Contact: JAnderson@winona.edu)

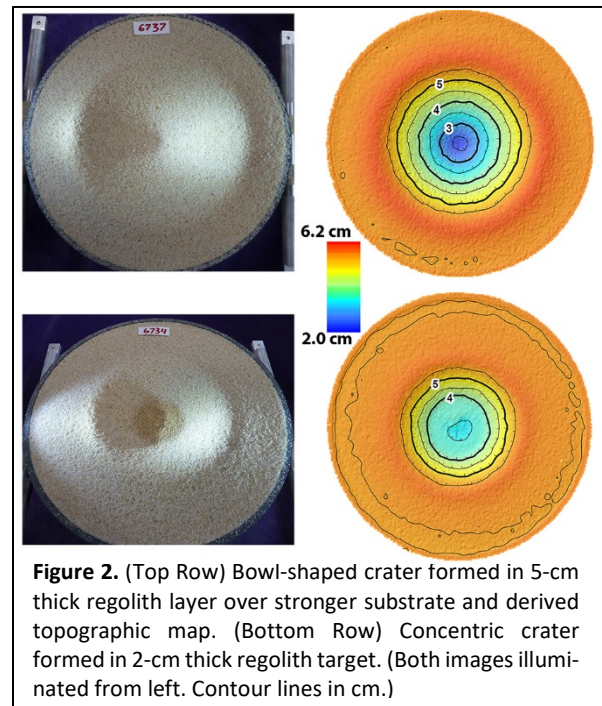
Introduction: Impact cratering is a fundamental physical process that has dominated the evolution and modification of nearly every planetary surface in the Solar System. Impact craters serve as a means to probe the subsurface structure of a planetary body and provide hints about target surface properties. By examining small craters on the lunar maria and comparing these to experimental impacts in the laboratory, Oberbeck and Quaide [1-2] first suggested that crater morphology can be used to estimate the thickness of a regolith layer on top of a more competent unit. Lunar craters show a morphological progression from a simple bowl shape to flat-floored and concentric craters (Fig. 1A) as crater diameter increases for a given regolith thickness. This quantitative relationship is commonly used to estimate regolith thicknesses on the lunar surface [3-8] and has also been explored via numerical [9-10] and experimental studies [11-13]. Here we report on a series of experimental impact craters formed in targets composed of a thin layer of loose sand on top of a stronger substrate (Fig. 1B) at the Experimental Impact Laboratory at NASA Johnson Space Center.



Experiment Design: Experimental impacts were performed in near-vacuum (< 1 torr) with 4.76-mm aluminum projectiles impacting the target at 1.54 km/s (\pm 0.02 km/s) and normal to the target surface. The “regolith” in these targets was a well-sorted quartz sand (0.4-0.8 mm grain size). The substrate was made of sand (grain size <0.5 mm) that was chemically bonded to represent a stronger unit (like a basalt flow) beneath the loose sand regolith (Fig. 1B). The thickness of the

regolith was varied from 0 to 5 cm. These impacts were compared to a control experiment that used a 12-cm deep target of the unbonded 0.4-0.8 mm sand.

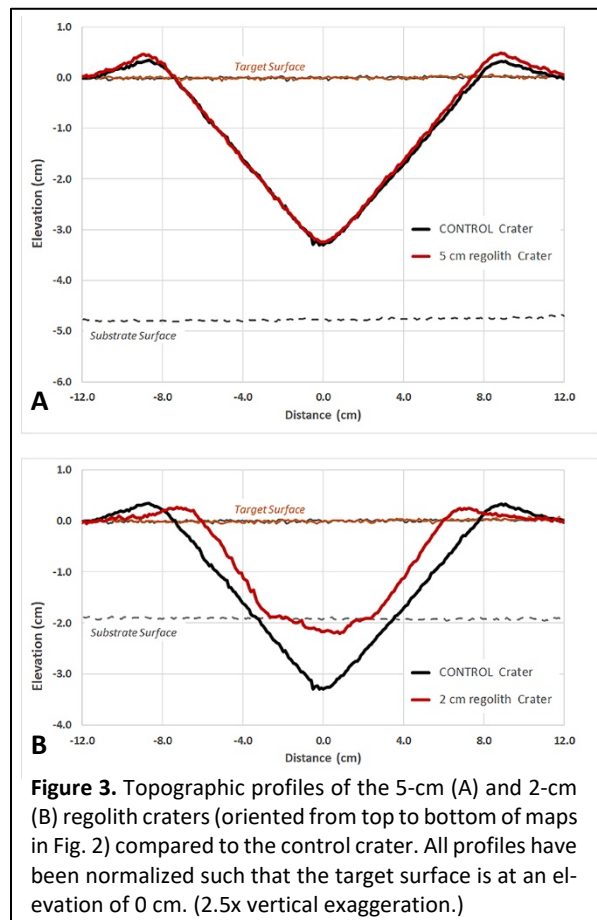
A NextEngine 3D scanner was used to record the target’s configuration before and after each experiment, permitting all crater measurements to be referenced to the pre-impact topography. Scans were also made of the substrate prior to the addition of the regolith such that the regolith thickness could be measured. The 3D scans were converted into topographic maps of the substrate, pre-impact target, and post-impact cratered surfaces. Each experiment was also imaged with the Ejection-Velocity Measurement System (EVMS) [14] allowing analysis of individual ejecta trajectories and derivation of crater- and ejection-speed scaling relationships. (Please see [12,13] and Anderson *et al.*, this conference [15], for our related discussion of the ejecta kinematics observed in these experiments.)



Initial Results: As an example, here we compare the craters formed into 2-cm and 5-cm thick layers of regolith with the control crater (Figs. 2 & 3). The 5-cm regolith crater was bowl-shaped and, at first glance, appeared to be a typical crater formed in sand (Fig. 3A) showing no interior features that might suggest a stronger substrate existed just below the thick regolith

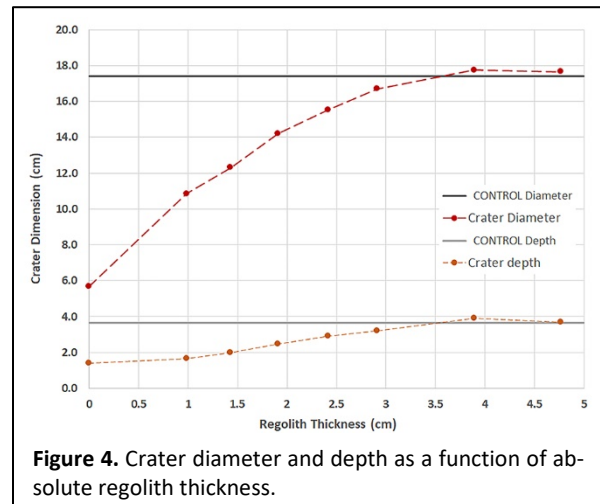
layer. Close comparison of the crater profile for the 5-cm regolith target with that of the control crater, however, shows a slightly thicker rim and a marginally wider crater. The slight difference in impact speed of the projectile for each experiment is not responsible for this difference – the projectile in the control experiment impacted at 1.572 km/s whereas that of the 5-cm regolith experiment was 1.524 km/s. This suggests that the slower impact into the 5-cm regolith layer formed a crater that is the same size, if not slightly larger, than the faster impact into the loose-sand only target. We will be examining this result in more detail with further experiments.

The 2-cm regolith crater, as expected, obviously was affected by the stronger substrate (Fig. 3B). It possessed a classic concentric morphology, with a cone-shaped profile in the regolith layer that was truncated at the surface of the substrate; it contained a smaller, central crater within the substrate itself.



Acknowledgements: This work would not have been possible without the EIL gunners Frank Cardenas and Roland Montes as well as Captain Electron, Terry Byers. And many thanks to Luke Zwiefelhofer and Nikki Schosow at Winona State. This work is supported by NASA SSW grant NNX16AR92G.

Discussion: Using the topographic maps of the final craters, we can measure various dimensions such as the standard rim crest-to-rim crest diameter, maximum crater depth, and rim height as well as dimensions of the various interior features including the diameter of the flat floor and the diameter of the central crater. An example of how the rim crest-to-rim crest diameter and crater depth vary with the thickness of the regolith layer is shown in Figure 4. As expected, craters generally become shallower and smaller as the regolith thickness decreases. However, there are subtle and important differences that can be seen in these high-resolution topographic maps and profiles. In particular, it seems that the stronger substrate affects the subsurface flow-field by redirecting material flow upward and outward resulting in a wider final crater shape even when the interface is still well below the crater floor (Fig. 3A).



We will continue to examine the relationships between crater morphometry and regolith thickness with high resolution topographic datasets. The additional insight from the ejecta kinematics analyses completed during these experiments [15] will further constrain our understanding of the subsurface flow-field during the formation of impact craters in strength-layered targets.

References: [1] Oberbeck & Quaide 1967, *JGR* **72**, 4697-4704. [2] Quaide & Oberbeck 1968, *JGR* **73**, 5247-5270. [3] Wilcox *et al.* 2005, *MAPS* **40**, 695-710. [4] Bart *et al.* 2011, *Icarus* **215**, 485-490. [5] Bart 2014, *Icarus* **235**, 130-135. [6] Di *et al.* 2016, *Icarus* **267**, 12-23. [7] Stopar *et al.* 2017, *Icarus* **298**, 34-48. [8] Yue *et al.* 2019, *Icarus* **329**, 46-54; [9] Senft & Stewart 2007, *JGR* **112**, E11002. [10] Prieur *et al.* 2018, *JGR* **123**, 1555-1578. [11] Dohi *et al.* 2012, *Icarus* **218**, 751-759. [12] Ebel *et al.* 2019, *LPSC* #2911. [13] Cline *et al.* 2019, *AGU* #3504. [14] Cintala *et al.* 1999, *MAPS* **34**. [15] Anderson *et al.* 2020, *LPSC*.